159. Structural Investigations of 13-*O*-Demethyl-FK506 and Its Isomers Generated by *in vitro* Metabolism of FK506 Using Human-Liver Microsomes

by **Wolfgang Schüler**[a]), **Uwe Christians**[b]), **P. Schmieder**[a]), **Hans-Martin Schiebel**[c]), **Ines Holze**[b]), **Karl-Friedrich Sewing**[b]), and **Horst Kessler**[a])*

[a]) Organisch-Chemisches Institut, Technische Universität München, Lichtenbergstr. 4, D-85748 Garching
[b]) Institut für Allgemeine Pharmakologie, Medizinische Hochschule Hannover, Konstanty-Gutschow-Str. 8, D-30625 Hannover
[c]) Institut für Organische Chemie, Technische Universität Braunschweig, Hagenring 30, D-38106 Braunschweig

(5.IV.93)

FK506 is currently under investigation as immunosuppressant after organ transplantation and in immune diseases. The structure of a demethylated metabolite **1** of FK506 isolated after *in vitro* metabolism by human-liver microsomes was established using two-dimensional homo- and heteronuclear NMR experiments. The demethylation position was found to be at *O*–C(13) using HMBC spectra. In contrast to FK506, 7 different isomers could be differentiated in COSY, HMBC, and HMQC spectra. The intensity of their signals was 50:18:11:9:6:6 (one isomer could not be quantified). This isomerization may be explained by epimerization at C(10) or alternative formations of the hemiketal ring between C(10) and C(13) or C(9) and C(13), in addition to *cis*/*trans*-isomerism about the amide bond (see *Scheme*). The structural variation is possible by participation of the OH group at C(13) formed after demethylation and could be derived from HMBC spectra. Chemical exchange evidenced by ROESY spectra proved the rotational isomerism. NMR investigation of the structure of 13-*O*-demethyl-FK506 (**1**) revealed at least seven isomers.

1. Introduction. – FK506 (tacrolimus, *Fujisawa*, Osaka, Japan) is currently under investigation as immunosuppressant after organ transplantation [1] and immune diseases [2] [3]. FK506 is isolated from *Streptomyces tsukubaensis* [4] and has a macrolide structure

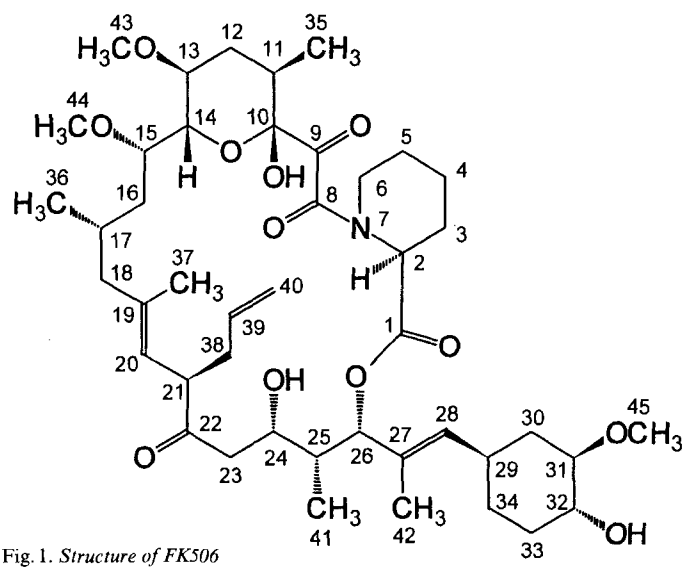

Fig. 1. *Structure of FK506*

($C_{44}H_{69}NO_{12}$) with a molecular mass of 803.5 Da (*Fig. 1*). FK506 is a 23-membered macrolide with a hemiketal-masked α,β-dioxocarboxamide. Its structure was established by NMR, X-ray crystal analysis, ozonolysis, and alkaline and acid hydrolysis [5]. The conformation in solution was determined by NMR and molecular-dynamics calculations [6].

FK506 is metabolized by enzymes of the cytochrome P450 3A subfamily [7] [8] to at least nine different metabolites [9]. The reactions involved are demethylation and hydroxylation. The immunosuppressive activity of the metabolites is reduced by demethylation to less than 10% of that of the mother compound [9]. Limited information of the *in vivo* metabolism in liver-graft patients is available showing the demethylated and di-demethylated FK506 metabolites in blood and urine using an HPLC/particle beam/MS technique [10]. The structures of 13-*O*-demethyl- [8] and 13,31-di-*O*-demethyl-FK506 [11] after *in vitro* metabolism were identified until now. The corresponding reports gave little information about different isomers of the metabolite and the assignment of the NMR spectra. It is the purpose of this work to evaluate the structure of the main FK506 metabolite by detailed analysis of its NMR spectrum.

2. Materials and Methods. – 1. *Generation and Purification of Demethyl-FK506* **1**. Demethyl-FK506 **1** was purified after metabolism by human-liver microsomes *in vitro* as described before [12]: Human-liver microsomes were isolated from a human liver with high cytochrome P450 3A4 content as estimated by semi-quantitative *Western* blotting using standard centrifugation techniques [13]. FK506 at a concentration of 10 μM in MeOH (1 mM) was mixed with 1 ml of microsomal suspension (in 0.1 mM phosphate buffer, pH 7.4, adjusted to 3 g protein/l) and 0.5 ml of an NADPH regenerating system consisting of 2 mM H_4edta, 10 mM $MgCl_2$, 0.84 mM NADP, 18 mM isocitric acid, and 667 U/l of isocitrate dehydrogenase and was incubated for 15 min at 37°. The reaction was stopped by addition of 0.5 ml of MeCN. The samples were centrifuged (2500 *g* for 2 min), and the supernatant was loaded on glass extraction columns filled with C_8-material (25–40 μm particle size). FK506 and its metabolites were purified with 3 ml of MeOH/H_2O pH 3.0 1:1 (*v*/*v*) and 1 ml of hexane. The extraction columns were set in 10-ml glass centrifuge tubes, and 1.5 ml of CH_2Cl_2 was centrifuged through the columns (450 *g*, 2 min). The eluates of *ca.* 2500 samples were pooled and the CH_2Cl_2 evaporated. The residue was dissolved in 10 ml of MeCN/H_2O pH 3.0 3:1 (*v*/*v*). The same volume of hexane was added and vortexed for 2 min, the hexane phase discarded, and a portion (200 μl) of the extract injected into a prep. HPLC system (*Hewlett-Packard 1084B* (*Hewlett-Packard*, Waldbronn, FRG), with *Merck-Hitachi-655A-40* autosampler, *655A* UV monitor, and *D-2000* integrator (*Merck*, Darmstadt, FRG); 250 × 10 mm *Nucleosil®-C_8* column (10 μm; *Macherey-Nagel*, Düren, FRG); MeCN/H_2O pH 3.0 (adjusted using H_2SO_4) 1:1 (*v*/*v*) as eluent, flow 5.0 ml/min; UV detection at 205 nm, column temp. 75°). FK506 and its metabolites were isocratically separated. Fractions of FK506 (t_R 18.3 min) and demethyl-FK506 (t_R 10.2 min) were manually collected, pooled, and extracted using an equal volume of CH_2Cl_2. For MS analysis, 10 ml of the CH_2Cl_2 phase was taken. The CH_2Cl_2 was evaporated, and the samples were dried under a stream of N_2 at 40° and subsequently under vacuum over P_2O_5: 9 mg (total yield) of demethyl-FK506 **1**. Purity of the sample was evaluated by negative direct chemical-ionization (CI) MS (*Finnigan-MAT-8430* mass spectrometer (*Finnigan-MAT*, Bremen, FRG), NH_3 as reactant gas; in *m*/*z*): 789 ([*M* – H]$^-$), 771 and 753 (thermically induced dehydration products), 586, 549, 489, 225; the isolated **1** was not contaminated by other FK506 derivatives.

2. *NMR-Measurement Conditions. General:* The basis of the assignment procedure was a set of 2D NMR spectra including P.COSY [14], TOCSY [15] [16], ROESY [17], HMQC [18] [19], DEPT-HMQC [20], HQQC [21], and HSQC [22] [23]. Furthermore, a HMQC-TOCSY [24] [25] with a short MLEV-17 pulse sequence of 10 ms, a ROESY with $(\pi\bar{\pi})_n$-spin-lock [26] to suppress TOCSY signals, and HMBC [27–30] were added. All NMR spectra were recorded at 300 K on a *Bruker-AMX500* spectrometer equipped with *X32* computers using the UXNMR software for data acquisition and calculation. A sample of **1** (3 mg; 7 mM) was dissolved in $CDCl_3$ (0.5 ml). The HMQC-TOCSY was recorded with a sample of **1** (6 mg; 15 mM) in $CDCl_3$ (0.5 ml) which was run through three freeze and pump cycles to remove O_2. For the HMBC, the *z*-filtered TOCSY, and $(\pi\bar{\pi})$-ROESY, a sample of **1** (9 mg; 22 mM) in $CDCl_3$ was used after three freeze and pump cycles to remove O_2.

1D ^{1}H-NMR Experiment: recorded with 16K data points and a spectral width of 5000 Hz and multiplied with a *Lorentz-Gaussian* function prior to transformation.

P.COSY: 500 MHz, 300 K. Sequence: D_1-90°-t_1-90°-t_2. Relaxation delay D_1 = 1.3 s, 4K data points in F_2 and 512 experiments in F_1, 8 scans, spectral width in both dimensions 5000 Hz (10.0 ppm). Apodization with a

$\pi/2$-shifted squared sine-bell function in both dimensions, phase-sensitive processing with zero-filling yielding a matrix of 4K × 1K complex points.

TOCSY: 500 MHz, 300 K. Sequence: D_1-90°-t_1-90°-*trim*-MLEV-17-*trim*-t_2. Relaxation delay D_1 = 1.3 s, MLEV-17 mixing sequence τ_{mix} = 100 ms with 2.5 ms *trim* pulses and a 9.5 kHz spin-locking field, 4K data points in F_2 and 512 experiments in F_1, 8 scans, spectral width in both dimensions 5000 Hz (10.0 ppm). Apodization with a $\pi/2$-shifted squared sine-bell function in both dimensions, phase-sensitive processing with zero-filling yielding a matrix of 2K × 1K complex points.

ROESY: 500 MHz, 300 K. Sequence: D_1-90°-t_1-90°-SL-90°-t_2. Relaxation delay D_1 = 1.3 s, SL = 4 kHz spin-lock with pulses of 1.5 µs and delays of 7.2 µs, during a mixing period of τ_{mix} = 120 ms; 4K data points in F_2 and 512 experiments in F_1, 8 scans, spectral width in both dimensions 5000 Hz (10.0 ppm). Apodization with a $\pi/2$-shifted squared sine-bell function in both dimensions, phase-sensitive processing with zero-filling yielding a matrix of 2K × 1K complex points.

HQQC: 500/125 MHz, 300 K. Sequence: D_1-90°(^{1}H)-Δ_1-180°(^{1}H)-180°(^{13}C)-Δ_1-90°(^{1}H)-Δ_2-90°(^{1}H)-Δ_1-180°(^{1}H)-90°(^{13}C)-Δ_3-90°(^{1}H)-$t_1/2$-180°(^{1}H)-$t_1/2$-90°(^{1}H)-180°(^{13}C)-Δ_1-180°(^{1}H)-90°(^{1}H)-Δ_4-t_2. Relaxation delay D_1 = 245 ms, Δ_2 = 3.57 ms, Δ_3 = 3.5211 ms, Δ_4 = 106.115 ms. 1K data points in F_2 and 128 experiments in F_1, 24 scans, spectral width in F_2 5000 Hz (10.0 ppm) and in F_1 10000 Hz (79.5 ppm). A second experiment used 4000 Hz (31.8 ppm) to yield a folding F_1 to enhance spectral resolution. Apodization with a $\pi/2$-shifted squared sine-bell function in both dimensions, phase-sensitive processing with zero-filling yielding a matrix of 2K × 1K complex points.

HMQC: with BIRD pulse sequence to suppress ^{1}H's connected to ^{12}C, 500/125 MHz, 300 K. Sequence: D_1-90°(^{1}H)-Δ_1-180°(^{1}H)-180°(^{13}C)-Δ_1-90°(^{1}H)-Δ_2-90°(^{1}H)-Δ_1-90°(^{13}C)-$t_1/2$-180°(^{1}H)-$t_1/2$-90°(^{13}C)-Δ_1-t_2. Relaxation delay D_1 = 245 ms, Δ_2 = 198 ms, Δ_1 = 3.57 ms; 1K data points in F_2 and 512 experiments in F_1, 16 scans, GARP decoupling during acquisition. Spectral width in F_2 5000 Hz (10.0 ppm) and in F_1 17857 Hz (142.0 ppm). Apodization with a $\pi/2$-shifted squared sine-bell function in both dimensions, phase-sensitive processing with zero-filling yielding a matrix of 2K × 1K complex points.

DEPT-HMQC: 500/125 MHz with BIRD pulse sequence and *z*-filter to suppress phase distortions, 300K. Sequence: D_1-90°(^{1}H)-Δ_1-180°(^{1}H)-180°(^{13}C)-Δ_1-90°(^{1}H)-Δ_2-90°(^{1}H)-Δ_1-90°(^{13}C)-Δ_1-180°(^{13}C)-$t_1/2$-180°(^{1}H)-$t_1/2$-Δ_3-90°(^{13}C)-Δ_4-90°(^{1}H)-Δ_5-90°(^{1}H)-t_2. GARP decoupling during acquisition, relaxation delay D_1 = 245 ms, Δ_1 = 3.57 ms, Δ_2 = 198 ms, Δ_3 = 3.5422 ms, Δ_4 = 3.621 ms, Δ_5 = 3 µs, 180° DEPT proton pulse to select positive signals for CH and CH_3 and negative signals for CH_2; 1K data points in F_2 and 512 experiments in F_1, 16 scans, spectral width in F_2 5000 Hz (10.0 ppm) and in F_1 17857 Hz (142.0 ppm). Apodization with a $\pi/2$-shifted squared sine-bell function in both dimensions, phase-sensitive processing with zero-filling yielding a matrix of 2K × 1K complex points.

HSQC: 500/125 MHz, 300K. Sequence: D_1-90°(^{1}H)-Δ_1-180°(^{1}H)-180°(^{13}C)-Δ_1-90°(^{1}H)-Δ_2-90°(^{1}H)-Δ_3-180°(^{1}H)-180°(^{13}C)-Δ_3-90°(^{1}H)-90°(^{13}C)-$t_1/2$-180°(^{1}H)-$t_1/2$-90°(^{1}H)-90°(^{13}C)-Δ_3-180°(^{1}H)-180°(^{13}C)-Δ_3-*trim*-t_2. Relaxation delay D_1 = 245 ms, Δ_1 = 3.57 ms, Δ_2 = 198 ms, Δ_3 = 1.785 ms, *trim* pulses of 2.5 ms, GARP decoupling during acquisition. 1K data points in F_2 and 512 experiments in F_1, 16 scans, spectral width in F_2 5000 Hz (10.0 ppm) and in F_1 17857 Hz (142.0 ppm). Apodization with a $\pi/2$-shifted squared sine-bell function in both dimensions, phase-sensitive processing with zero-filling yielding a matrix of 2K × 1K complex points.

HMQC-TOCSY: with BIRD pulse to suppress ^{1}H's connected to ^{12}C, 500/125 MHz, 300K. Sequence: D_1-90°(^{1}H)-Δ_1-180°(^{1}H)-180°(^{13}C)-Δ_1-90°(^{1}H)-Δ_2-90°(^{1}H)-Δ_1-180°(^{13}C)-$t_1/2$-180°(^{1}H)-$t_1/2$-90°(^{13}C)-Δ_1-*trim*-MLEV-17-*trim*-t_2. Relaxation delay D_1 = 168.5 ms, Δ_1 = 3.57 ms, Δ_2 = 227.5 ms, GARP decoupling during acquisition; 2K data points in F_2 and 1K experiments in F_1, 128 scans, spectral width in F_2 4032 Hz (8.1 ppm) and in F_1 19230 Hz (152.9 ppm). Apodization with a $\pi/2$-shifted squared sine-bell function in both dimensions, phase-sensitive processing with zero-filling yielding a matrix of 2K × 1K complex points.

HMBC: with low pass filter, 500/125 MHz, 300K. Sequence: D_1-90°(^{1}H)-Δ_1-90°(^{13}C)-Δ_2-90°(^{13}C)-$t_1/2$-180°(^{1}H)-$t_1/2$-180°(^{13}C)-Δ_3-90°(^{13}C)-t_2. Relaxation delay D_1 = 1.35 s, Δ_1 = 3.57 ms, Δ_2 = 60 ms, Δ_3 = 25 µs; 8K data points in F_2 and 512 experiments in F_1, 328 scans, spectral width in F_2 4274 Hz (8.5 ppm) and in F_1 18519 Hz (147.2 ppm). Folding of the F_1 dimension at 145.09 ppm. Apodization with a $\pi/2$-shifted squared sine-bell function in both dimensions, phase-sensitive processing with zero-filling yielding a matrix of 2K × 1K complex points. Magnitude calculation in F_2. Strong T_1 noise was reduced using the *Aurelia* program.

TOCSY: with *z*-filter, 500 MHz, 300K. Sequence: D_1-90°-t_1-Δ-DIPSI-Δ-90°-t_2. The DIPSI sequence consisted of pulses which were derived from the 90° pulses with the factors 3.555, 4.555, 3.222, 3.1666, 0.333, 2.722,

4.166, 2.944, and 4.111. Relaxation delay D_1 = 1.35 s, spin-lock (mixing time) 90 ms, 8 different delays from 5 μs to 4 ms were used for the z-filter delay Δ per increment, 4 scans, 8 K data points in F_2, 512 experiments, spectral width 4274 Hz (8.5 ppm) in F_2 and F_1. Apodization with a $\pi/2$-shifted squared sine-bell function in both dimensions, phase-sensitive processing with zero-filling yielding a matrix of 2 K × 1 K complex points.

ROESY: with suppression of scalar coupling with a $(\pi\bar{\pi})_n$ spin-lock sequence, 500 MHz, 300 K. Sequence: D_1-90°-t_1-180$_\phi$°-(180$_{-\phi}$°-180$_\phi$°)$_n$-t_2. Relaxation delay D_1 = 3.0 s, mixing time 400 ms, 8 K data points in F_2, 512 experiments in F_1, 72 scans, spectral width 5051 Hz (10.10 ppm) in F_2 and F_1. Apodization with a $\pi/2.5$-shifted squared sine-bell function in both dimensions, phase-sensitive processing with zero-filling yielding a matrix of 2 K × 1 K complex points.

Results. – 1. *Assignment of NMR Spectra.* A comparison of the NMR spectra of demethyl-FK506 **1** with those of the parent compound showed a lot of changes in the chemical shifts and additional signals indicating the presence of at least seven different isomers. Because of such profound differences, a completely new assignment was required. In analogy to FK506, *cis/trans*-isomerism about the amide bond was expected for the metabolite. As demethylation induced changes in the chemical shifts in different regions of the molecule, obviously the conformation of the macrolide ring was changed as well. It had to be evaluated whether the additional signals were associated with conformational isomers, metabolites with different demethylation positions, or impurities. It could be shown that the sample was contaminated by proton-rich material among which the plastic softener dioctyl phthalate could be identified.

The chemical shifts of ^{1}H- and ^{13}C-NMR resonances of **1** are listed in *Table 1*. Besides the data of the major isomer **1a**, *Table 1* also contains those of minor isomer populations (**1b–g**, different in the region C(18) to C(28); **1iii–vi**, different in the region C(2) to C(8); **1III–IV**, different in the region C(11) to C(16); **1**δ, **1**ε, and **1**φ, different in the region C(18) to C(21)) which could be discriminated by NMR. Assignment showed five regions of the molecule where various numbers of isomers could be distinguished. In the region C(1) to C(8), five isomers could be detected, in the region of C(11) to C(16) at least four, and in the region of C(18) to C(28) at least seven. The moieties C(30) to C(33) and C(40) revealed only one set of signals (*Table 1*).

Table 1. *Assignment of the ^{1}H- and ^{13}C-NMR Chemical Shifts of 13-O-Demethyl-FK506* (**1**) *in $CDCl_3$ at 300 K*[a])

	Major isomer **1a**		Other isomers[b])		
	δ (H)	δ (C)		δ (H)	δ (C)
C(1)		169.4	**1b**		170.0
			1c		169.9
			1d		169.5
			1e		170.8
			1f		168.4
H–C(2)	5.17	51.8	**1b**	4.77	56.5
			1iii	4.50	57.0
			1iv	5.10	52.1
			1v	5.23	54.0
			1vi	4.49	56.2
CH_2(3)	1.74, 2.29	26.0	**1b**	1.80, 2.30	27.0
			1iii	1.61, 2.09	
			1iv	1.55, 2.32	25.9
			1v	1.80, 2.31	26.1

Table 1 (cont.)

	Major isomer **1a**		Other isomers[b])		
	δ (H)	δ (C)		δ (H)	δ (C)
CH_2(4)	1.41, 1.77	21.0	**1b**	1.40[c]), 1.74[c])	21.0
			1iii		21.1
			1iv	1.35[c]), 1.71[c])	20.6
			1v		21.0
CH_2(5)	1.51, 1.64	24.6	**1b**	1.47, 1.70	
			1iii	1.49, 1.61	
			1iv	1.51, 1.59	
CH_2(6)	3.20, 3.45	44.8	**1b**	2.82, 4.46	39.7
			1iii	2.94, 4.46	41.4
			1iv	3.01, 4.46	44.1
			1v		44.7
C(8)		166.6	**1b**		165.3
			1iii		164.9
			1iv		166.8
			1v		166.6
C(9)		200.1	**1b**		193.3
C(10)		104.2	**1b**		105.2
					106.5[c])
H–C(11)	2.92	42.6	**1b**	2.59	39.0
			1III	2.57[c])	
CH_2(12)	1.78, 2.44	32.3	**1b**	1.76, 2.20	32.1
			1III	1.80, 2.49	34.1
H–C(13)	4.39	82.3	**1b**	4.27	80.9
			1III	4.31	80.8
H–C(14)	3.79	72.9	**1b**	3.53	73.2
			1III	3.48	
H–C(15)	3.23	79.6	**1b**	3.09	79.2
			1III	3.27	79.2
			1IV	3.37	77.7
CH_2(16)	1.15, 1.68	36.0	**1b**	1.08, 1.60	36.0
			1III	1.28, 1.66	36.7
			1IV	1.25, 1.74	35.7
H–C(17)	1.86	27.2			28.4
CH_2(18)	1.97, 2.02	48.2	**1b**	1.84, 2.02	48.8
			1c	1.83, 2.06	46.7
			1δ		48.2
			1ε		46.2
			1φ		47.0
C(19)		139.2	**1b**		139.0
			1c		139.8
H–C(20)	5.06	122.4	**1b**	4.89	123.6
			1c	4.90	122.5
			1d	4.93	123.1
			1ε	4.88	123.6
			1φ	4.97	123.2
H–C(21)	3.31	53.4	**1b**	3.28	52.6
			1c	3.36	52.7
			1d	3.33	53.4
			1ε	3.30	52.5
			1φ		52.6
C(22)		211.4			

Table 1 (cont.)

	Major isomer **1a**		Other isomers[b])		
	δ (H)	δ (C)		δ (H)	δ (C)
CH_2(23)	2.63, 2.73	44.2	**1b**	2.57, 2.68	46.2
			1c	2.51, 2.74	45.3
			1d	2.56, 2.67	45.0
H–C(24)	3.86	69.0	**1b**	4.03	69.2
			1c	4.15	67.6
			1d	3.95	70.1
			1e	3.87	69.7
			1f	3.95	68.5
H–C(25)	1.85	39.4	**1b**	1.74	38.6
			1c	1.70	38.5
			1d	1.84	39.8
			1e	1.71	39.9
			1f	1.80	39.1
H–C(26)	5.16	80.0	**1b**	5.31	80.7
			1c	5.21	82.0
			1d	5.13	80.1
			1e	5.12	79.2
			1f	5.02	81.7
			1g	5.21	77.0
C(27)		131.0	**1b**		131.0
			1c		133.0
			1f		132.9
H–C(28)	5.18	130.9	**1b**	5.17	130.9
			1c	5.27	132.9
			1d	5.01	131.3
			1e	5.13	131.2
			1f		131.1
H–C(29)	2.27	34.7	**1b**	2.27	34.7
			1c	2.25	34.6
			1d	2.27	
CH_2(30)	0.96, 2.01	34.4			
H–C(31)	2.98	84.0			
H–C(32)	3.37	73.3			
CH_2(33)	1.34, 1.97	31.0			
CH_2(34)	1.07, 1.57	30.4	**1b**		30.5
			1c		30.3
Me(35)	1.01	12.6	**1b**	1.09	13.2
			1c	1.07[c])	
Me(36)	0.91	21.5	**1b**	0.94	21.1
			1c	0.92	20.3
			1δ	0.95	
			1ε	0.88	
			1φ	0.89	
Me(37)	1.70	17.3	**1b**	1.72	17.0
			1c	1.73	18.9
			1d	1.72[c])	17.2
			1ε	1.71	16.9
			1φ	1.69	17.0
CH_2(38)	2.18, 2.45	34.8	**1b**	2.12, 2.45	34.6
H–C(39)	5.67	135.4	**1b**	5.67	135.4
			1c		135.3
CH_2(40)	4.96, 5.03	116.5			

Table 1 (cont.)

	Major isomer **1a**		Other isomers[b])		
	δ (H)	δ (C)		δ (H)	δ (C)
Me(41)	0.90	8.8	**1b**	0.81	6.8
			1c	0.87	8.5
			1d	0.90	8.8
			1e		9.3
			1f		9.4
Me(42)	1.57	13.4	**1b**	1.58	13.8
			1c	1.60	12.2
			1d	1.61	13.9
			1e		13.4
			1f		12.8
Me(44)	3.34	57.5	**1b**	3.31	57.1
			1III	3.39	57.7
			1IV	3.39	57.9
Me(45)	3.39	56.3			

[a]) The chemical shifts are given in relation to $CDCl_3$ (δ (H) 7.24 ppm, δ(C) 77.0 ppm).

[b]) The designations of the minor isomers are different in some spin systems (**1b–f**, **1iii–vi**, **1III–IV**, **1δ–φ**) since not all sets of signals could be cross-referenced between the spin systems. The signals of minor isomers are indicated by the same symbol as far as they can be assigned to the same isomer. Therefore, it may be possible that different symbols represent the same isomer.

[c]) These values are tentatively assigned.

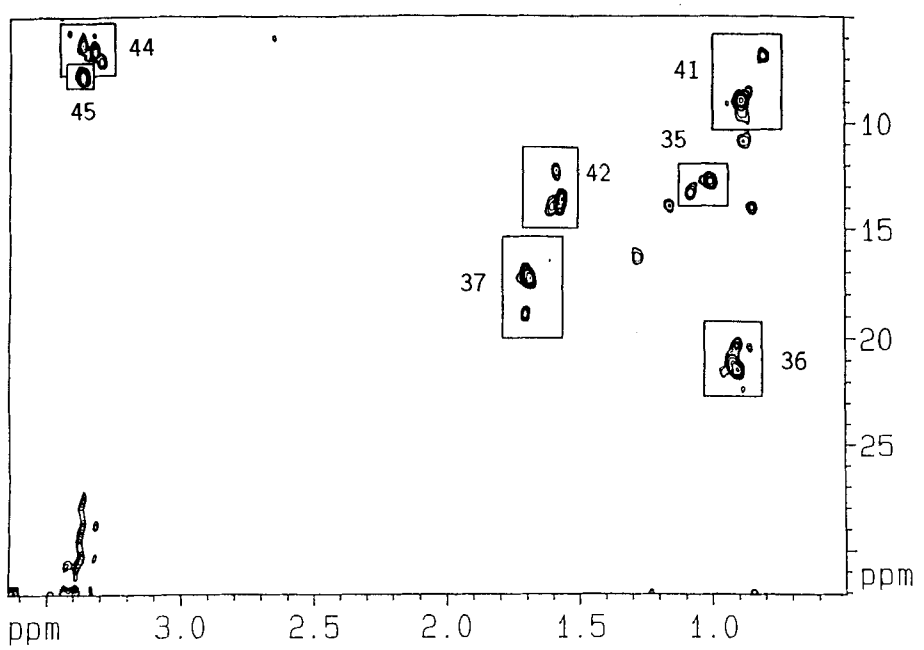

Fig. 2. *2D-HQQC* (500 MHz, 300 K) *of 13-* O-*demethyl-FK506* (**1**). The signals of the Me groups (C(44), C(45)) are folded. Signals of the same groups stemming from different isomers are included in boxes. As derived from TOCSY correlations, the signals outside the boxes are not associated with FK506 metabolites and are most likely caused by interfering impurities of the sample.

One of the main problems was to discriminate the multiple overlapping ^1H signals and their connections to respective isomers. This could only be achieved by using the combination of homonuclear and heteronuclear experiments to resolve overlapping ^1H signals in the dimension of the ^{13}C chemical shifts. The position of the MeO groups were identified by HQQC (heteronuclear quadruple quantum correlation) experiments. Only Me groups can form heteronuclear quadruple quantum correlations and are thus selected in this experiment. Two groups of signals could be differentiated (*Fig. 2*), the MeO groups being clearly discriminated from the other Me groups by their downfield shifts of H- and C-atoms. Assignment and identification of the spin systems C(2) to C(6), C(11) to C(18), C(20) to C(40), C(23) to C(26), and C(28) to C(34), which were separated from each other by quarternary C-atoms, was accomplished as previously described for FK506 [6]. The connectivities between the spin systems were analyzed using ROE's and HMBC spectra.

For the discrimination between conformers and constitutional isomers, COSY, HMBC, and HMQC experiments were used, since only few spin systems of the minor isomer populations could be identified by TOCSY due to interferences. The HMBC experiment with the high number of 328 scans per experiment in the F_1 dimension was

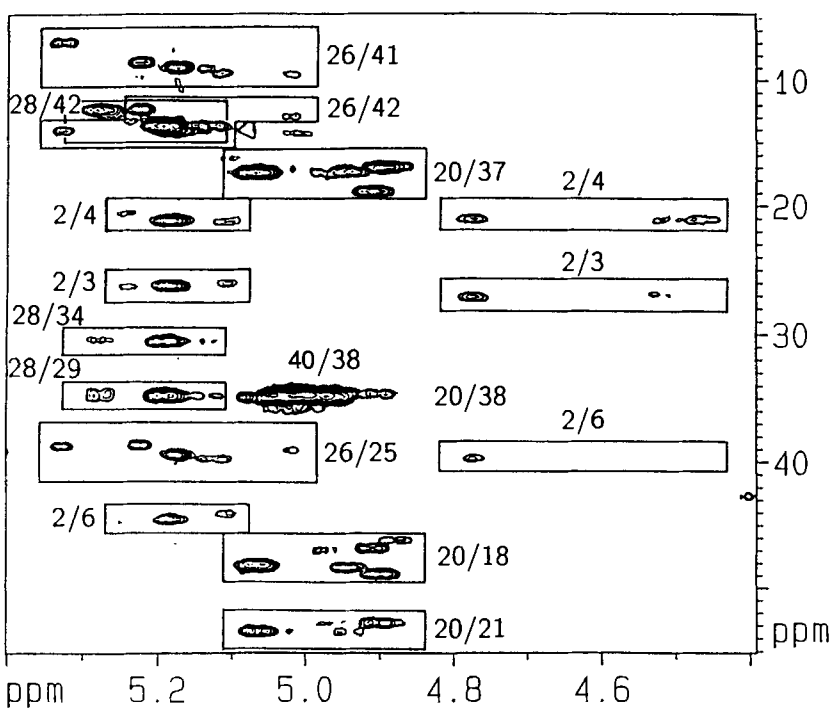

Fig. 3. *Segment of the HMBC* (500 MHz, 300 K) *of 13-O-demethyl-FK506* (**1**). Identification of *H*–C(26) using heteronuclear correlations with C(41), C(42), and C(25) as well as of *H*–C(20) *via* C(21), C(18), and C(37). The first value shows the assignment in F_2, and the second one in F_1. *H*–C(2) shows signals related to C(3), C(4), and C(6). Furthermore, signals of the different isomers can be discriminated. The wide differences of the chemical shifts of the isomers are evident, especially for *H*–C(2). The low-field signals of *H*–C(2) corresponds to the *trans*-conformation of the amide bond.

sensitive enough to allow the identification of signals from minor populated isomers. These signals were identified using the following connectivities: H–C(26)/C(24), H–C(26)/C(25), H–C(26)/C(41), H–C(26)/C(42), and H–C(26)/C(28) (see *Fig. 3*). Here the splittings in both dimensions were relatively large, and multiple redundancies of the signals allowed a specific discrimination. The isomers were named **1a–f** in the order of decreasing signal intensities starting with the major isomer **1a** (see *Table 1*). The connection of the different ^{1}H-spin systems *via* correlation to C(22) was only possible for isomers **1a–d**. Minor populated isomers in the region C(18) to C(21) were called **1δ**, **1ε**, and **1φ** since their association with isomers **1d**, **1e**, and **1f** could not clearly be established. Only **1a** and **1b** could be identified *via* correlation to C(17). At C(15) and C(16), only four, and at C(14) to C(11), only three isomers were visible. It could not be differentiated how the isomers **1a–g** as well as **1δ**, **1ε**, and **1φ** contributed to these signals.

Conformational flexibility was already observed in FK506 [6]. In the metabolite studied, the dynamic effects obviously resulted in an averaging of the signals of the cyclohexyl side chain, *i.e.* C(29) to C(34) and C(45) of the different isomers.

In the HMBC experiment, H–C(2) allowed correlations to C(3), C(4), C(2)/C(6) (*via* N(7)), C(1), C(8) (*Fig. 3*). The respective ^{1}H- and ^{13}C-shifts of H–C(2) for the isomers were found to be rather different. Two groups of signals, H–C(2) of **1a**, **1iv**, and **1v**, and H–C(2) of **1b**, **1iii**, and **1vi**, could be distinguished (boxes in the lower left corner of

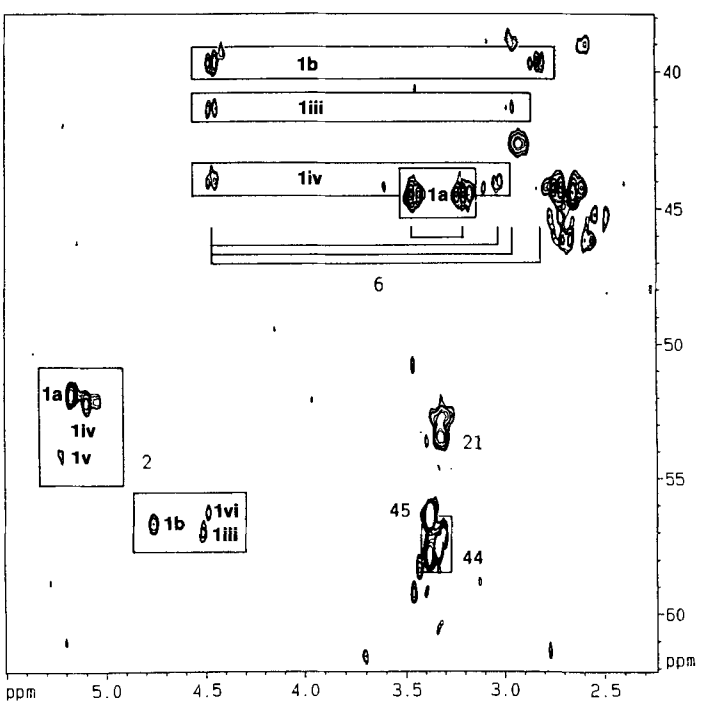

Fig. 4. *Segment of the HMQC* (500 MHz, 300 K) *of 13-O-demethyl-FK506* (**1**). Bottom: The H–C(2) signals of the different isomers allow to distinguish two groups which could be affiliated to *cis*/*trans*-isomerism. Top: Signals of 2 H–C(6).

Fig. 4). Assignment of *H*–C(2) of **1b** was proven by the ROE signal of this *H*–C(2) to Me(41) of **1b**, which was detected in an isolated position at the highest-field shift (not shown). Accordingly, CH_2(23), *H*–C(28), *H*–C(24), and CH_2(12) of **1b** could be assigned by ROE's using this Me(41).

The relative populations of the different isomers detected was roughly estimated using signal intensities of *H*–C(26) and *H*–C(24) of the isomers in the HMQC experiment. The following ratio was found: **1a**/**1b**/**1c**/**1d**/**1e**/**1g** 50:18:11:9:6:6; isomer **1f** could not be quantified.

2. *Identification of the Demethylation Position.* In the region of C(18) to C(11), all connectivities were proven by COSY signals. In FK506, this region contained Me(43)O and Me(44)O and C(13) and C(15). From *H*–C(13) as well as from *H*–C(15), an ROE to a MeO group at 3.34 ppm could be detected. A clear discrimination of the MeO signals of **1** was possible using an HMBC experiment. Separated cross-peaks could be observed between the protons of Me(44) and C(15) for the isomers **1a**, **1b**, **1III**, and **1IV** (*Fig. 5a*, top). The Me(45)/C(31) correlation resulted in an intense cross-peak with overlapping signals of the isomers, which could not be distinguished. This could be attributed to the relative flexibility of the side chains which cancelled different chemical shifts of the isomers. No cross-peaks could be detected between MeO protons and C(13). Those peaks were usually detectable in the range of 80.8–82.3 ppm for the other C-atoms (*Fig. 5a*, bottom).

This result was confirmed by correlating *H*–C(15) and C(44) for **1a**, **1b**, **1III**, and **1IV**. The correlation *H*–C(31)/C(45) showed, as expected, only one intense cross-peak. However, no correlation between C(43) and *H*–C(13) for any of the isomers could be found (*Fig. 5b*).

Since the 2 MeO groups at C(15) and C(31) as well as the other 5 Me groups were detected, while no evidence for the existence of a MeO group at C(13) was found, the loss of this MeO group and formation of an OH group at C(13) during the metabolism of FK506 by cytochrome P450 3A4 could be established.

3. *Conformers of 13-*O*-Demethyl FK506* (**1**) *and Comparison of the Chemical Shifts with Those of FK506 and Rapamycin.* In analogy to FK506, the metabolite **1** was also expected to form *cis*/*trans*-rotamers about the amide bond in $CDCl_3$. As the exchange of *cis*/*trans*-isomers occurs in the typical chemical-shift time scale of the NMR experiment [31], this equilibrium could be proven using ROESY experiments. The exchange signals in ROESY differ from cross-peaks in their sign [32]. However, they have to be distinguished from signals resulting from scalar coupling, which have the same sign as the exchange signals and the diagonal signals. Only few proton resonances (*H*–C(2), CH_2(6), *H*–C(11)) show differences between the conformers wide enough to result in detectable exchange signals, apart from the diagonal. In the ROESY spectra, *H*–C(2) (**1a**/**1b**) and *H*–C(2) (**1iii**/**1iv**) could be found.

The isomers of **1** showed prominent chemical-shift differences, especially for the moiety near the amide bond N(7)–C(8). *H*–C(2) showed two groups of signals in the range of 5.1–5.23 and 4.5–4.77 ppm (*Table 1*). A similar effect could be observed for *H*–C(11) (2.92 *vs.* 2.59 and 2.57 ppm), although less isomers were distinguishable. The protons at C(6) also showed prominent differences of the chemical shifts and the extent of diastereotopic splitting. These effects were influenced by the conformation about the amide bond and allowed qualitative differentiation of the *cis*/*trans*-conformers. In *Table*

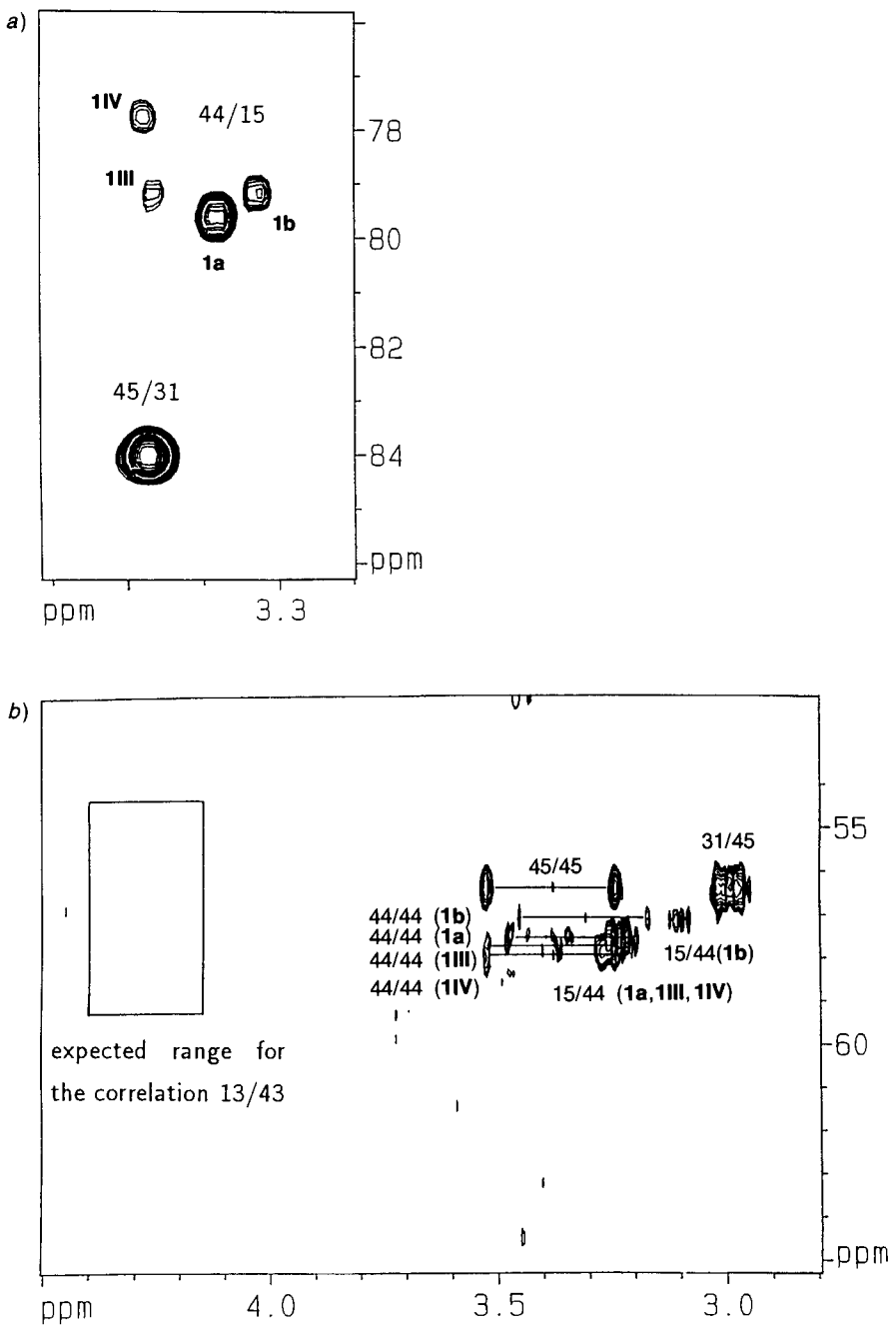

Fig. 5. *Segment of the HMBC* (500 MHz, 300 K) *of 13-*O*-demethyl-FK506* (**1**). a) *Correlation of the MeO protons with three-bonds-distant C-atoms, which allowed the assignment of the MeO groups.* b) *Correlation of the MeO C-atoms with three-bonds-distant protons.*

2, these shifts are compared with FK506 and the structurally related immunosuppressive macrolide rapamycin [33] (the chemical shifts of rapamycin in $CDCl_3$ are unpublished data).

Table 2. NMR Differentiation ($CDCl_3$) *of* cis- *and* trans-*Rotamers about the Amide Bond of 13-*O*-Demethyl-FK506* (**1**) *and Comparison with the Characteristic Chemical Shifts of FK506* [6] *and Rapamycin* [33]

	Rapamycin			FK506		13-*O*-Demethyl-FK506					
	trans[a])	*trans*	*cis*	*trans*	*cis*	**1a**, *trans*	**1b**, *cis*	**1iii**, *cis*	**1iv**, *trans*	**1v**	**1vi**
C(2)	50.8	51.3	56.2	52.7	56.6	51.8	56.5	57.0	52.1	54.0	56.2
H–C(2)	4.91	5.29	4.29	4.94	4.53	5.17	4.77	4.50	5.10	5.23	4.49
C(6)	43.5	44.2	39.1	43.9	39.2	44.8	39.7	41.4	44.1	44.7	
H_{ax}–C(6)	3.15	3.44	3.22	3.14	2.98	3.20	2.82	2.94	3.01		
H_{eq}–C(6)	3.41	3.58	4.44	3.68	4.36	3.45	4.46	4.46	4.46		

[a]) In (D_6)DMSO.

Differentiation of the *cis*/*trans*-conformers, *i.e.* of the major isomers **1a** and **1b**, was similar to that of FK506. In the case of **1iv**, the shifts of H_{eq}–C(6) and H_{ax}–C(6) were not evident; analysis of the more characteristic ^{13}C shifts showed *trans*-configuration of the amide bond of **1iv**. Accordingly, *trans*- and a *cis*-configuration was assumed for **1v** and **1iii**, respectively. Comparison of the ^{1}H-NMR chemical shifts of both FK506 conformers with the two main isomers **1a** and **1b** of 13-*O*-demethyl-FK506 showed clearly, that demethylation at *O*–C(13) had an extended effect on the conformation structure involving the whole molecule. The most striking differences were detected around the demethylation position (*H*–C(13)) and surprisingly at *H*–C(23) (see *Fig. 6*). By demethylation at *O*–C(13) and formation of an OH function, *H*–C(13) and the low-field *H*–C(23) of **1a**

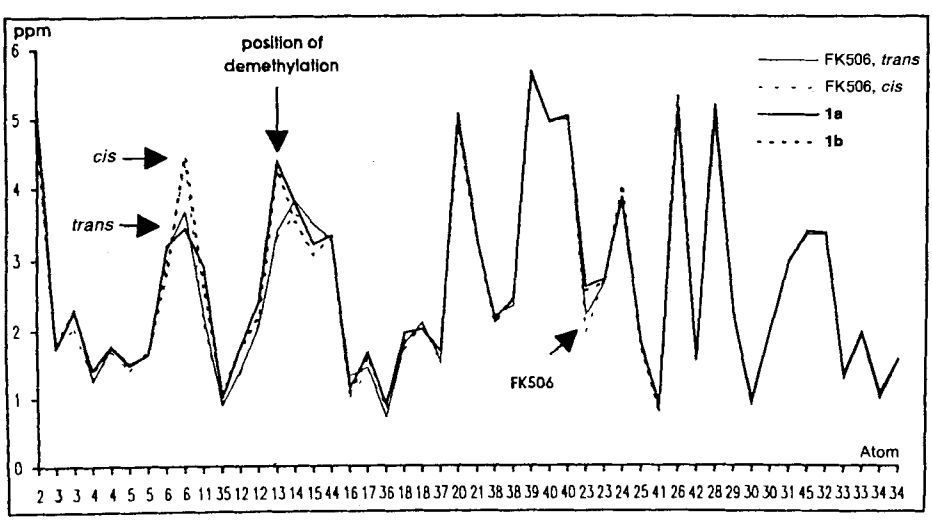

Fig. 6. *Plot of the ^{1}H-NMR chemical shifts of the two FK506 conformers and the two major isomers* **1a** *and* **1b**. In the case of CH_2 groups, the low-field shifted proton was plotted first.

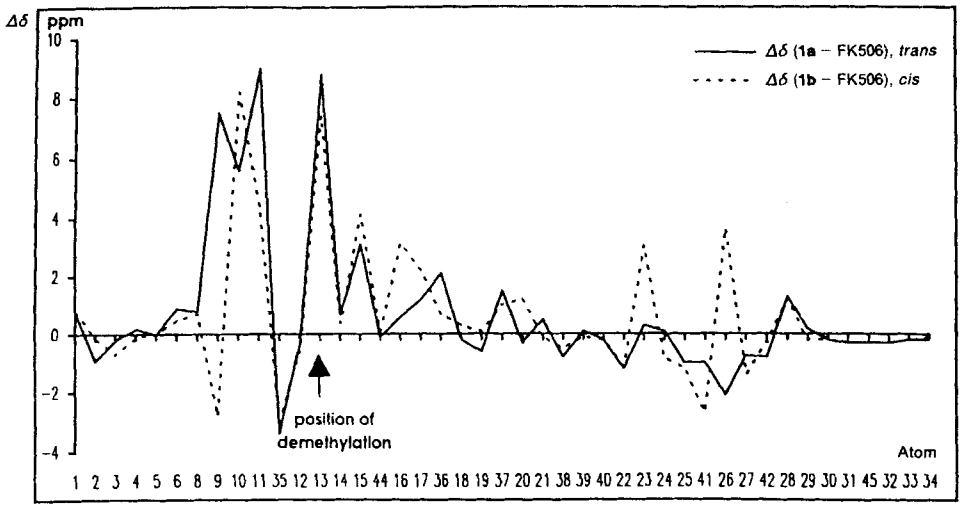

Fig. 7. *Comparison of the differences of the* ^{13}*C-NMR chemical shifts* ($\Delta\delta$) *between the* trans*-rotamer of FK506 and* **1a** *and the* cis*-isomer of FK506 and* **1b**

and **1b** were deshielded in comparison with FK506. Compared with the *trans*- and *cis*-conformers of FK506, the ^{13}C-NMR chemical shifts of **1a** and **1b** displayed changes in the regions C(9) to C(15), around the demethylation position C(13), and in the region of C(23) to C(28) (*Fig. 7*).

4. *Constitutional Isomers of 13-*O*-Demethyl FK506.* The observation of numerous isomers of **1** can be explained by the assumption of constitutional isomers. In combination with *cis/trans*-isomerism, 12 different species can be postulated (see *Scheme*: **A**, **C**, **D**, and **E** for the *trans*-isomers). The possible formation pathways are proposed in the *Scheme*. The hemiketal function at C(10) (see **A**) can be cleaved during the process of metabolism leading to **B** and subsequent formation of alternative ring structures and consecutive stereochemical changes.

The configuration at C(10) of **1** can only indirectly be derived. One of the main arguments was that exchange signals of H–C(2) were only detected for the isomers **1a**/**1b** and **1iv**/**1iii**. This could be explained by two different rotamers of the amide bond and two different configurations at C(10). A ring closure of **B** alternative to **B** → **C** could produce a furan-ring isomer **D** (two diastereoisomers). HMBC Experiments showed indeed a significant correlation between H–C(13) and C(10) of isomer **1a**. A possible correlation H–C(14)/C(10) could not be distinguished from the noise level. This may be interpreted as formation of a furan ring in which H–C(13) and C(10) are separated by only three bonds in *trans*-isomer **1a** and *cis*-isomer **1b**. In the same way, a reaction involving C(9)=O with formation of a six-membered hemiketal ring is possible (→ **E**, two diastereoisomers).

The complexity of the spectra with numerous overlaps, even in heteronuclear correlations, in addition to the small intensity of some isomer signals, prevented an unambiguous identification of all signal sets.

Scheme. *C(2) to C(14) Moiety of 13-O-Demethyl-FK506* (**1**): *Species* **A**–**E**[a])

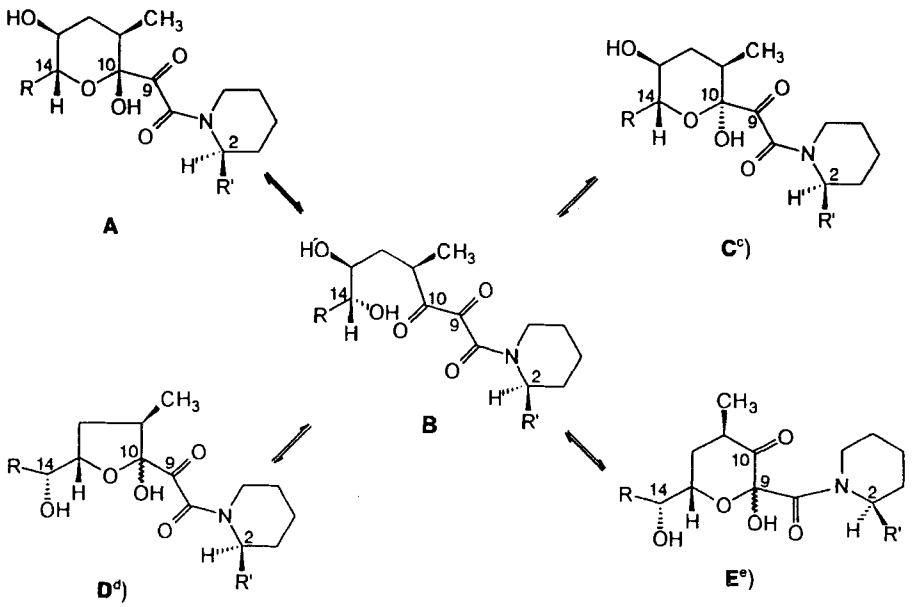

[a]) Opening of the hemiketal **A** at C(10) (→ **B**) and closure of the ring can change the configuration at C(10) (→ **C**). Alternative ring formations from **B** can bind OH–C(13) to C(10) (→ **D**) or C(9) (→ **E**), each leading to two stereoisomeric hemiketals.

Discussion and Conclusions. – *In vitro* metabolism of FK506 by human-liver microsomes lead to cleavage of Me(43) of the MeO group at C(13) and subsequent formation of an OH function. Although *Iwasaki et al.* [11] reported demethylation at *O*–C(13) and *Vincent et al.* [8] formation of the furan ring and *cis*/*trans*-rotamers, indirectly assumed from HPLC analysis, the authors did not describe neither constitutional isomers of 13-*O*-demethyl-FK506 (**1**) nor a complete assignment of NMR spectra. It could now be demonstrated that during the process of metabolism, the six-membered hemiketal ring was destabilized leading to alternative ring formations affecting the conformation of other regions of the molecule. Based upon NMR data, the formation of these isomers are rationalized. Additionally to these constitutional isomers, as for FK506, *cis*/*trans*-rotamers about the amide bond were present. Seven different isomers were detected, and the ^{1}H- and ^{13}C-NMR chemical shifts were assigned for all isomers as far as possible. The major isomer **1a** (*trans*) and consequently the corresponding *cis*-isomer **1b** showed a furan-ring structure, including a connection between C(10) and C(13).

There was only indirect information about the configuration at C(10). A confirmation of the isomer structures requires complete evaluation of the structure including constitution, configuration, and conformation. This seems impossible to accomplish by use of the non-isotopically labelled metabolite 13-*O*-demethyl-FK506 (**1**) due to the heavily overlapping signals in certain regions of the spectra.

FK506 in $CDCl_3$ shows *cis*/*trans*-isomerism in NMR but no constitutional isomers. In cyclosporine, a cyclic undecapeptide which is currently the main immunosuppressant

to prevent graft rejection after organ transplantation, the ring structure is not changed during metabolism. As shown in this study, the situation with 13-*O*-demethyl-FK506 (**1**) and presumably with other FK506 metabolites is far more complicated compared with cyclosporine, and it remains to be evaluated in how far destabilization and isomerism of the hemiketal ring structure involving C(10) influences the biologic and toxic activity of FK506 metabolites.

The authors want to thank Mrs. *R. Schottmann* and Ms. *A. Linck* for their skilful technical assistance and Dr. *M. Kobayashi*, *Fujisawa*, Osaka, Japan, and Dr. *A. Möller*, *Fujisawa*, Munich, Germany, for the FK506 sample. The study was supported by the *Deutsche Forschungsgemeinschaft* as well as the *Fonds der Chemischen Industrie*.

REFERENCES

[1] T.E. Starzl, S. Todo, J. Fung, A.J. Demetris, R. Venkataramanan, J. Ashok, *Lancet* **1989,** *ii*, 1000.
[2] K. Abu-Elmagd, D. Van Thiel, B.V. Jegasothy, C.D. Ackerman, S. Todo, J.J. Fung, A.W. Thomson, T.E. Starzl, *Transplant. Proc.* **1991,** *23*, 3322.
[3] M. Mochizuki, K. Masuda, T. Sakane, G. Inaba, K. Ito, M. Kogure, N. Sugino, M. Usui, Y. Mizushima, S. Ohno, Y. Miyanaga, S. Hayasaka, K. Ohizumi, *Transplant. Proc.* **1991,** *23*, 3343.
[4] T. Goto, T. Kino, M. Nishiyama, M. Okuhara, M. Koshsaka, H. Aoki, H. Imanaka, *Transplant. Proc.* **1987,** *19*, 4.
[5] H. Tanaka, A. Kuroda, H. Marusawa, *J. Am. Chem. Soc.* **1987,** *109*, 5031.
[6] D.F. Mierke, P. Schmieder, P. Karuso, H. Kessler, *Helv. Chim. Acta* **1991,** *74*, 1027.
[7] M. Sattler, F.P. Guengerich, C.Y. Yun, U. Christians, K.-F. Sewing, *Drug Metab. Dispos.* **1992,** *20*, 753.
[8] S.H. Vincent, B.V. Karanam, S.K. Painter, S.H.L. Chiu, *Arch. Biochem. Biophys.* **1992,** *294*, 454.
[9] U. Christians, C. Kruse, R. Kownatzki, H.M. Schiebel, R. Schwinzer, M. Sattler, R. Schottmann, A. Linck, V.M.F. Almeida, F. Braun, K.-F. Sewing, *Transplant. Proc.* **1991,** *23*, 940.
[10] U. Christians, F. Braun, M. Schmidt, N. Kosian, H.M. Schiebel, L. Ernst, M. Winkler, C. Kruse, A. Linck, K.-F. Sewing, *Clin. Chem.* **1992,** *38*, 2025.
[11] K. Iwasaki, T. Shiraga, K. Nagase, K. Hirano, K. Nozaki, K. Noda, *Transplant. Proc.* **1991,** *23*, 2757.
[12] U. Christians, H.H. Radeke, R. Kownatzki, H.M. Schiebel, R. Schottmann, K.-F. Sewing, *Clin. Biochem.* **1991,** *24*, 271.
[13] F.P. Guengerich, 'Principles and Methods of Toxicology', Ed. A.W. Hayes, Raven Press, New York, 1982, pp. 609.
[14] D. Marion, A. Bax, *J. Magn. Reson.* **1988,** *80*, 528.
[15] M.H. Levitt, R. Freeman, T. Frenkiel, *J. Magn. Reson.* **1982,** *47*, 328.
[16] A. Bax, D.G. Davis, *J. Magn. Reson.* **1985,** *65*, 355.
[17] A. Bax, D.G. Davis, *J. Magn. Reson.* **1985,** *63*, 207.
[18] L. Müller, *J. Am. Chem. Soc.* **1979,** *101*, 4481.
[19] A. Bax, R.H. Griffey, L.B. Hawkins, *J. Magn. Reson.* **1983,** *55*, 301.
[20] H. Kessler, P. Schmieder, M. Kurz, *J. Magn. Reson.* **1989,** *85*, 400.
[21] H. Kessler, P. Schmieder, M. Köck, M. Reggelin, *J. Magn. Reson.* **1991,** *91*, 375.
[22] G. Bodenhausen, D.J. Ruben, *Chem. Phys.* **1980,** *69*, 185.
[23] A. Bax, M. Ikura, K.E. Kay, D.A. Torchia, R. Tschudin, *J. Magn. Reson.* **1990,** *86*, 304.
[24] H. Kessler, W. Bermel, C. Griesinger, presented at the '6th Meeting of the Section Magnetische Resonanzspektroskopie', Berlin, September 25–28, 1985.
[25] L. Lerner, A. Bax, *J. Magn. Reson.* **1986,** *69*, 375.
[26] T.L. Hwang, A.J. Shaka, *J. Am. Chem. Soc.* **1992,** *114*, 3157.
[27] A. Bax, M.F. Summers, *J. Am. Chem. Soc.* **1986,** *108*, 2093.
[28] W. Bermel, K. Wagner, C. Griesinger, *J. Magn. Reson.* **1989,** *83*, 223.
[29] M.F. Summers, L.G. Marzilli, A. Bax, *J. Am. Chem. Soc.* **1986,** *108*, 4285.
[30] H. Kessler, P. Schmieder, M. Köck, M. Kurz, *J. Magn. Reson.* **1990,** *88*, 615.
[31] H. Kessler, *Angew. Chem.* **1970,** *82*, 237; *ibid. Int. Ed.* **1970,** *9*, 219.
[32] H. Kessler, M. Gehrke, C. Griesinger, *Angew. Chem.* **1988,** *100*, 507; *ibid. Int. Ed.* **1988,** *27*, 490.
[33] H. Kessler, R. Haessner, W. Schüler, *Helv. Chim. Acta* **1993,** *76*, 117.